EUROPEAN FUSION DEVELOPMENT AGREEMENT

EFDA–JET–PR(01)116

E.Lazzaro et al

Error Field Locked Modes Thresholds in Rotating Plasmas, Anomalous Braking and Spin-up

Error Field Locked Modes Thresholds in Rotating Plasmas, Anomalous Braking and Spin-up

E.Lazzaro[1],R.J.Buttery[2],T.C.Hender[2],P.Zanca[3],R.Fitzpatrick[7],M.Bigi[2],T.Bolzonella[3],
R.Coelho[6], M.DeBenedetti[4],S.Nowak[1],O.Sauter[5],M.Stamp[2]
and contributors to the EFDA-JET workprogramme*

[1]Istituto di Fisica del Plasma del CNR, Assoc. EURATOM-ENEA-CNR per la Fusione, Via R.Cozzi 53, Milan,Italy
[2]EURATOM/UKAEA Fusion Assoc.Culham Science Centre, Abingdon,Oxon-OX14 3DB, UK
[3]CONSORZIO RFX Assoc. EURATOM-ENEA-CNR per la Fusione, C.so Stati Uniti 4, Padova Italy
[4]CRE ENEA Assoc. EURATOM-ENEA per la Fusione, Via E. Fermi 7, Frascati, Italy
[5]CRPP / EPFL Assoc. EURATOM-Switzerland, Lausanne, Switzerland
[6]Associaçã EURATOM/IST, Centro de Fusão Nuclear, 1096 Lisbon,CODEX, Portugal
[7]Institute for Fusion Studies, Department of Physics, University of Texas at Austin, Austin TX 78712
** See annex of J. Pamela et al, "Overview of Recent JET Results and Future Perspectives", Fusion Energy 2000 (Proc. 18th International Conference on Controlled Fusion and Plasma Physics, Sorrento, 2000), IAEA, Vienna (2001)*

Paper to be submitted for publication in Physics of Plasmas

ABSTRACT

The mechanisms of nonlinear interaction of external helical fields with a rotating plasma are investigated analyzing the results of recent systematic experiments on JET that widen the previous data base collected on Compass-D, DIII-D and JET. The empirical scaling laws governing the onset of "error field" locked modes are re-assessed and interpreted in terms of existing driven reconnection theories and with new models. In particular the important mechanism of plasma rotation braking and spin up associated with error fields are analyzed in detail and interpreted.

I. INTRODUCTION.

The ideal tokamak configuration of nested toroidal isobaric magnetic surfaces desired for plasma confinement, is well known to be susceptible to non axisymmetric magnetic perturbations that are resonant with closed field line surfaces. On dissipative time scales even an ideally stable plasma can respond to imperfections of the magnetic geometry that tear the ideal configuration deteriorating particles and energy confinement and leading frequently to disruption of the discharge. In addition error field locked modes can be seed neoclassical tearing modes (NTMs) and lead to a limit to high β_p performance.

Therefore it is important to understand the appearance of resistive locked magnetic islands caused by the helical component of unavoidable "error fields" . The basic mechanism to be understood is the non-linear response of magnetic reconnection at rational-q surfaces driven by resonant "error-fields" and the possible screening effect provided by plasma rotation. There have been a number of experimental studies [1-4] of locked modes driven by error fields showing this screening effect implies a threshold in error field amplitude to form a locked mode.

These comments anticipate the motivation of the systematic work undertaken recently on the JET device [5] to widen existing data bases on the subject, that is relevant for the ITER design [6], with the aim, in particular, to establish the threshold of the amplitude of external helical magnetic fields as function of the main plasma equilibrium parameters. The appropriate scaling laws are identified including as a novel feature the dependence on the plasma toroidal rotation frequency (ω_0).

Further motivation comes from the comparison of the effects of "externally" driven modes with those resulting from "spontaneous" reconnection. Namely it has long been known [7], but not yet explained, that the onset of locked modes often has a strong "non-local" effect on the plasma toroidal rotation profile. This aspect is related to the "anomalous" nature of the perpendicular plasma viscosity as well as to the possible appearance of a toroidal viscous force due to broken axisymmetry [8].

The paper is organized into a Section presenting the set-up of the JET experiment, a description of the data analysis employed to obtain the threshold power laws , in comparison with the best known theoretical models and previous results from other experiments. The following Section discusses the limitations of conventional models and points out the discrepancies with the experimental observations, isolating the key questions to be addressed. The third and fourth Sections contain the

outline and a discussion of possible models for the anomalous plasma braking and spin-up. The last section gives conclusions and perspectives for the understanding and controlling realistic forced reconnection phenomena in tokamak experiments and fusion devices.

II. ACTION AND RESPONSE EXPERIMENTS WITH HELICAL ERROR FIELDS ON JET

The flexibility of the JET device has been used to improve the understanding of the response of tokamaks to very small accidental ("error") external field perturbations that are generally observed to lock rotating modes causing rapid amplitude growth to disruptive conditions on a variety of tokamaks [1-4,7,10].

The JET tokamak is fitted, within the vacuum vessel, with a system of saddle coils (see Fig.1) that can be fed with variable polarity by an appropriate power supply and controller, and were originally meant to test concepts of electro-dynamic feedback control of tearing modes [11]. The objective of the work presented here is however to single out as much as possible the essential physics of the linear and non-linear reconnection response on the basis of systematic experiments in which a DC external helical field having a large component with poloidal and toroidal pitch numbers (m =2, n=1) is applied by the saddle coils (Fig.2)

Previous experimental results and a number of theoretical arguments indicate that when the amplitude of the static external perturbation resonant at a certain q=m/n surface exceeds a critical value, the driven linear reconnection process bifurcates, leading to a non-linearly amplified state forming a magnetic island. The onset of this non-linear stage is commonly referred to as "penetration" of the external field perturbation, in partial analogy with the phenomenon of penetration of a time varying magnetic field into a conductor [2,12] although in the case considered here the characteristic time scales are hybrid expressions involving electrical resistive times, inertial times and fluid viscous times. For a fixed aspect ratio R/a and safety factor $q_a = aB_\varphi / RB_\theta$, the dependence of the normalized threshold value for penetration b_{pen}/B on plasma parameters can be expected to be represented by a power law scaling $b_{pen}/B \propto n^{a_n} B^{a_B} T_e^{a_T} P_{aux}^{a_P}$ where n is the plasma density, B the toroidal field, T_e the electron temperature and P_{aux} the auxiliary,non-Ohmic power density.

According to similarity principles applied to tokamaks [16] the operational independent variables are B and P_{aux}, From the point of view of both the theoretical models of forced reconnection and tokamak operation it is preferable to investigate a scaling of the form $b_{pen}/B \propto n^{a_n} B^{a_B} \omega_0^{\eta}$ that involves explicitly the density and the plasma rotation frequency, which is related to a condition of local competition of the electro-dynamic and viscous torques that oppose reconnection [12]. In the initial stage of the field penetration the plasma velocity deviates strongly from the equilibrium profile only in the vicinity of the rational surface. The observed rotation is really in the toroidal direction, as in the poloidal direction the phase velocity of the perturbation, coincident with that of the plasma trapped in the island is strongly damped by the neoclassical viscous force. The toroidal rotation is most frequently observed to be in the electron drift direction (opposite to direction of the plasma equilibrium current), hereafter to be labeled as "positive" direction. The application of

external torque, via Neutral Beam Injection or external fields may alter in either way the rotation direction.

The experiments on JET considered here were performed in plasmas with low power neutral beams (NBI) momentum injection, operating at constant q_{95}~3.5 with the toroidal field B in the range from 1 to 3 T, and with densities in the range 1.4 – 3.3 10^{19} m^{-3} in a Single Null separatrix configuration (see Table I). A slow ramp of "error' field is applied (Fig.3a) with the helical component m=2, n=1 reaching an amplitude of $B_{2,1} \approx 6.5 \cdot 10^{-4} T$ at the q=2 surface. As apparent from Fig.3b, 3c the amplitude ramp of the magnetic perturbation produces an electro-dynamic torque that brakes the toroidal plasma rotation at the q=2 surface located at the major radius position $R_{q=2} = 3.7$ m and when the local angular rotation frequency $\omega_0 \equiv \omega(R = R_{q=2}, t_0)$ has been reduced to a critical value $\omega \approx \omega_0/2$ (Fig.3c) the initially linear driven response, measured in the laboratory frame by a set of peripheral magnetic pick-up coils, is non-linearly amplified (Fig.3b). The start time of the coils current ramp is t_0. This indicates field penetration and formation of a magnetic island, that is subsequently "locked" as shown on the temperature profile measured by ECE (Electron Cyclotron Emission), in Fig.4. When the external field is switched off and the natural error field is suitably compensated (Fig.3a), the locked mode is observed to spin up either in the e- or the i- drift direction (Fig.3b) because of viscous restitution of momentum from the underlying plasma flow.

The scaling of the threshold on density and field is related to the underlying dependence of the rotation on those variables; this is a machine-dependent aspect of the problem that needs being sorted out with some care for specific experimental conditions. For the shots at constant P_{NBI} multiple regression on the data leads to the scaling $b_{pen}/B \propto n^{0.97\pm0.05} B^{-1.2\pm0.06}$ in line with that found previously on JET [3] in absence of rotation. With NBI momentum injection of power P_{NBI} the rotation frequency scales as $\omega_0 \propto B^{\alpha} \left(P_{NBI}/n\right)^{\beta}$ in agreement with previous observations in JET discharges with NBI power input [7]. Multiple regression analysis of the data gives for the rotation frequency the power law scaling displayed in Fig.5 with exponents $\alpha \cong 0.56, \quad \beta \cong 0.63$. Furthermore it is observed that the density depends on B as $n \propto B^{0.3}$. Theory predicts different scaling of the threshold with frequency depending on the prevalent dissipative regimes [12,13]. In the so called *visco-resistive* regime defined by the condition $\omega_0 << \omega_I \cong \tau_V^{1/3} \tau_R^{-2/3} \tau_H^{-2/3}$, where the time constants appearing in the definitions are $\tau_V = a^2/\mu_\perp$ the anomalous perpendicular viscous time of the order of the energy confinement time, $\tau_R = \mu_0 a^2/\eta$ the resistive diffusion time and $\tau_H = a/v_A$, the Alfvén time.

In this regime' *expected* dependence of b_{pen}/B on frequency is linear [4,5] and the best fit of the data with this assumption is $b_{pen}/B \propto n^{0.55\pm0.03} B^{-1.25\pm0.03} \omega_0$ as displayed in Fig.6. A much better fit is given by $b_{pen}/B \propto n^{0.58\pm0.02} B^{-1.274\pm0.02} \omega_0^{0.5}$ (Fig.7).

The non-linear scaling with ω_0 is in agreement with the scaling in the *ideal viscous* regime [12] defined by $\omega_0 > \omega_I$. This implies that the effective (anomalous) viscous time should have values of the order of $\tau_V \approx \tau_R^2 \tau_H^2 \omega_0^3 \approx 10^{-2}$ s.

We can actually argue that the scaling shown in Fig. 7 is the most consistent and physically meaningful. It should be recalled that in absence of rotation the threshold scaling is

$b_{pen}/B \propto n^{a_{n0}} B^{a_{B0}}$ with $a_{n0} = 0.97$, $a_{B0} = -1.207$. Since $\omega_0 \propto B^{\alpha}/n^{\beta}$, then $b_{pen}/B \propto n^{a'_n} B^{a'_B} \omega_0^{0.5}$ with $a'_n = a_{n0} + 0.5\beta = 1.285$ and $a'_B = a_{B0} - 0.5\alpha = -1.487$. Considering that for the present data $n \propto B^{0.3}$ and that the data regression of Fig.7 gives $a_n = 0.58$, one can write $a_B = a'_B + 0.3(a'_n - a_n) = -1.275$ and obtain $b_{pen}/B \propto n^{0.58} B^{-1.275} \omega_0^{0.5}$ that shows a remarkable consistency of the present results with those obtained in absence of rotation [4].

In Table II a summary of results of different previous experiments and some theoretical predictions is presented for comparison.

The analysis of the data shows substantial agreement with the empirical scaling of the threshold of the field penetration found in previous experiments on JET (see Table II) and supports the view that externally driven magnetic reconnection at rational-q surfaces is contrasted by plasma rotation, which is therefore beneficial. However behind the global result of this experiment much more complex physics is hidden that need to be discussed in detail. The process appearing as a nonlinear "penetration" of the external field, with consequent island formation, has been studied in detail in Ref [12] within a Rutherford regime [14] and is associated with the torque balance conditions that may occur in a viscous plasma subject to electrodynamic forces.

The experiments confirm strikingly the fact that as the threshold for nonlinear reconnection is reached the rotation frequency is approximately one half of its initial value, according with the formula

$$\frac{\omega}{\omega_0} = \frac{1}{2} + \frac{1}{2}\left[1 - \left(\frac{b_{ext}}{b_{thres}}\right)^2\right]^{1/2} \qquad (1)$$

as shown in Fig.8 for a single discharge (52067) and in Fig.9 for a group of discharges.

This interpretation is consistent with a picture of the islands' motion in the plasma fluid similar to that of a rigid body, with no net plasma flow across the separatrix [2,12]. In a single fluid plasma model this "no slip" constraint leads to the assumption that the flux surface averaged deviations of the fluid (poloidal and toroidal) angular velocities $\Delta\omega_{\theta,z}(r)$ from the "natural" values due to a single magnetic island be hindered by perpendicular viscosity and therefore governed by a diffusion equation with suitable conditions on axis and at the edge. In steady state the resulting toroidal velocity shift is then expected to be rigid body like between the axis and the inboard radius of the of the island separatrix (roughly $0 \le r \le r_s$) and sheared for larger radii [12].

The evidence provided by the JET experiments, as well as that of other machines is however in contrast with this idealized picture and requires a new point of view that will be described in the next paragraphs. The main observation, presented in Fig.3c and in Figs.10,11,12 is that as the non-linear mode amplification ("penetration") takes place, the toroidal velocity profile $V_\varphi(r,t) = \omega(r,t)R$ collapses everywhere self-similarly, which is incompatible with a viscous decay. In detail Fig.3c shows a superposition of the magnetic pick-up coils signal monitoring the growth of the m=2, n=1 signal and the traces of the charge exchange measurement (CXSM) of plasma rotation. The CXSM traces giving the time history of rotation at all radii are visibly collapsing together at the onset of the

non-linear reconnection (at t =18.4 s from the start of the discharge); thus the braking appears sudden and uniformly across the plasma cross section. The rotation frequency is normalized to the value at the starting time point of the "error field" ramp. The interpretation of this fact is not trivial, as it appears also from the CXSM plots of the radial rotation profiles with superposition of the (2,2) (3,2) and (1,1) rational surfaces identified by the EFIT magnetic reconstruction code ; Fig.10 shows for shot 52067 that during the subcritical part of the external field ramp, $t< t_{ric}$ (Fig.3a) a seemingly diffusive slow reduction of velocity occurs, with clear localization of the braking torque at the resonant radius of the (2,1) surface. At† "field penetration" time the braking is abrupt and distributed across the whole plasma body.

More precisely as apparent from Fig.11, for shot 52067, and in Fig.12 for several discharges, the no-slip condition on the variation of toroidal angular frequency $\Delta\omega(r) \equiv \left(\omega(r,t) - \omega_0(r_s)\right) \cong \text{const.}$ for $0 < r < r_{q=2}$ [2,12] is *not* met, the variation being larger in the central part than near the q=2 surface where the torque has a resonant peak. No other resonant torque appears to influence the rotation profile at other rational surfaces so the direct effect of a mode coupling mechanism seems unlikely in this case.

Data for shot 52061 (Fig.13) show that after the instant in which the coils have been switched on (t_{start}), there is a quite long phase in which *only* the q=2 (R=3.7) surface undergoes a significant braking. This is interpreted as the effect of the localized electromagnetic torque which develops at this surface. The global braking of the plasma velocity happens rapidly, associated with the reconnection of the q=2 surface.

Thus the characteristics of the braking observed are not diffusive and indeed an analysis of the scaling of the observed braking rate suggests that the anomalous rotation damping can be described by

$$d\left[V_\varphi(r,t)/V_0(r)\right]/dt = -\left|b_\theta/B_0\right|^\alpha \nu_{0\varphi} V_\varphi(r,t)/V_0(r) \qquad (2)$$

associated with some mechanism depending on the field perturbation as $\left|b_\theta\right|^\alpha$, with a close to 2. In Eq. 2 $\nu_{0\varphi}$ is an appropriate damping coefficient.

A nonlinear MHD problem for the m=2,n=1 mode has been solved numerically for a plasma of constant density, rotating toroidally with an initial velocity profile $V_0(r)$ and with boundary conditions that include an external helical current field perturbation I_E. The resistive MHD equations:

$$\frac{\partial \mathbf{B}}{\partial t} + \nabla \wedge [\mathbf{v} \wedge \mathbf{B}] = \tfrac{\eta}{\mu_0}\nabla^2 \mathbf{B} - \nabla \tfrac{\eta}{\mu_0} \wedge \nabla \wedge \mathbf{B} \qquad (3)$$

$$\rho \frac{d\mathbf{v}}{dt} = -\nabla p + \mu_0 \nabla \wedge \mathbf{B} \wedge \mathbf{B} + \mu_\perp \nabla^2 \mathbf{v} \qquad (4)$$

(where ρ is the mass density, $\eta(r)$ the resistivity and $\mu_\perp$ the perpendicular viscosity) have been solved in a customary RMHD model in the tokamak ordering, where the equilibrium and perturbed magnetic and velocity fields $\mathbf{B} = \mathbf{B}_0(r) + \mathbf{b}(r,\theta,\varphi,t)$ and $\mathbf{v} = V_{0\varphi}(r,t)\hat{\mathbf{e}}_\varphi + \mathbf{v}_\perp(r,\theta,\varphi,t)$ are represented through flux and stream functions [14] in the form

$$\mathbf{B} = B_{0z}\mathbf{e}_z + B_{0\theta}\mathbf{e}_\theta + \sum_{m,n} \nabla \wedge \left(C_{m,n} \psi^{m,n} e^{i\left(m\theta - nz/R + \varphi_{m,n}\right)} \mathbf{e}_{m,n} \right)$$

and

$$\mathbf{v} \cong V_{\varphi 0}(r,t)\mathbf{e}_z + \sum_{m,n} \nabla \wedge \left(C_{m,n} \phi^{m,n} e^{i\left(m\theta - nz/R + \varphi_{m,n}\right)} \mathbf{e}_{m,n} \right)$$

with suitable direction vectors and metric coefficients tied to the m,n helical path on a cylinder of radius r.

Up to four (complex) harmonics of the flux and stream functions are considered and each harmonic is governed by Reduced MHD equations obtained from Eqs. (2,3) and also the background toroidal plasma velocity and equilibrium poloidal magnetic field are evolved in time by the quasi-linear equations

$$\rho_0 \frac{\partial V_{\varphi 0}}{\partial t} = \frac{1}{2R_0} \sum_{m,n} \frac{n}{\mu_0} Im\left(\psi^{*m,n} \nabla^2 \psi^{m,n} \right) - n\rho_0 Im\left(\phi^{*m,n} \nabla^2 \phi^{m,n} \right) + \mu_\perp \nabla^2 V_{\varphi 0}$$

$$\frac{\partial \psi_0}{\partial t} = -\frac{1}{2} \sum_{m,n} \frac{m}{r} \frac{\partial}{\partial r} Im\left(\phi^{m,n} \psi^{*m,n} \right) + \frac{\eta}{\mu_0} \nabla_0^2 \psi_0 + E_0$$

The numerical simulation of the driven reconnection problem with a simple viscous damping of the toroidal rotation is performed using a finite difference scheme over a suitable non-uniform radial grid and a two step implicit-explicit method in time [15]. Even though this model goes beyond the constant y approximation of the Rutherford regime [14], it leads to a result in substantial agreement with the "no–slip" expectation. As shown in Fig.14 the non-linear amplification ("penetration") of the helical flux $Re[\psi(r)e^{i(m\theta - nz/R)}]$ occurs when $V_\varphi = V_{\varphi 0}/2$ and the *variation* of the velocity profile $\Delta V_\varphi(r,t) = \Delta\omega(r,t) \cdot R$ shown in Fig.15 tends to be pretty much uniform. The inadequacy of the diffusive model and a qualitative agreement of model (2) with the observations is shown in Figs. 15 and 16 with $|b_\theta|^2$ for $(m \neq 0, n \neq 0)$,or $|b_\varphi|^2$ for $(m = 0, n \neq 0)$for the reasons explained in next section.

The discrepancy with the experimental observations and the scaling of the braking rate suggest a conjecture on additional braking mechanisms linked to the radial and helical structure of the perturbation. As discussed below in detail the breaking of axisymmetry due to resonant and non-resonant helical field perturbations can in fact give origin, in general, to a toroidal viscous force, normally identically zero in axisymmetry [17].

III. NEOCLASSICAL VISCOUS FORCE

The neoclassical toroidal viscous force [8,17] is a good candidate to explain the global braking of the plasma rotation. This effect is present in non-axisymmetric plasmas only, and in our case it could appear when the magnetic perturbation induced by the saddle coils become important. Its flux-surface averaged expression is [17]

$$\left\langle e_\phi \cdot \nabla \cdot \Pi \right\rangle = \frac{2\pi^{1/2} p_i}{v_{Ti}} V_\phi \sum_{m,n\neq 0} \left\langle \frac{e_\phi \cdot \nabla B}{B} \frac{\partial b^{m,n}}{\partial \phi} \right\rangle \frac{q}{|m - nq|} \qquad (5)$$

where p_i is the ion pressure, v_{Ti} is the ion thermal speed and B is the magnetic field magnitude, whose perturbations are denoted $b^{m,n}$:

$$B(r,\theta,\phi) = B_0(r)\left(1 + \sum_{m,n\neq 0} b^{m,n}(r,\theta,\phi)\right) \tag{6}$$

The notation m,nπ0 means that the toroidal and poloidal mode numbers cannot be simultaneously zero. In (5) we have discarded a term proportional to the plasma poloidal velocity, under the assumption of a strong poloidal flow damping. All the resonant and non-resonant magnetic perturbations produced by the saddle coils must be taken into consideration in (5), including the m=0 component. For this reason we have to model the magnetic perturbation in the plasma to higher order than usual in the aspect ratio $\varepsilon = r/R$. To this purpose it is convenient to adopt the notation developed in [19] for a cylindrical plasma with periodicity 2 pR in the z direction. In this case f=z/R is a simulated toroidal angle and the equilibrium magnetic field $\mathbf{B}_0 = \left(0, B_{0\theta}(r), B_{0\phi}(r)\right)$ and current $\mathbf{J}_0$ are related by the force balance equation $\mathbf{J}_0 \times \mathbf{B}_0 = \nabla P_0$ and AmpËre's law $\nabla \times \mathbf{B} = \mu_0 \mathbf{J}$ that give

$$\nabla \times \mathbf{B}_0 = \mu_0 \frac{\mathbf{J}_0 \cdot \mathbf{B}_0}{B_0^2}\mathbf{B}_0 - \mu_0 \frac{\nabla P_0 \times \mathbf{B}_0}{B_0^2} \tag{7}$$

Defining the pressure gradient and the parallel current density profile as

$g(r) = \frac{\mu_0}{B_0^2}\frac{dP_0}{dr}$ and $\sigma(r) = \mu_0 \frac{\mathbf{J}_0 \cdot \mathbf{B}_0}{B_0^2}$ equation (7) gives

$$\mu_0 \mathbf{J}_0 = \left(0, \sigma B_{0\theta} + g B_{0\phi}, \sigma B_{0\phi} - g B_{0\theta}\right) \tag{8}$$

The linearized form of the curl of the force balance equation determines the perturbed field $\mathbf{b}$

$$(\mathbf{b}\cdot\nabla)\mathbf{J}_0 - (\mathbf{J}_0\cdot\nabla)\mathbf{b} + (\mathbf{B}_0\cdot\nabla)\mathbf{j} - (\mathbf{j}\cdot\nabla)\mathbf{B}_0 = 0 \tag{9}$$

Introducing direction vectors $\mathbf{e}_{m,n} = C_{m,n}(0, n\,r/R, m)$ tied to the m,n helical path on a cylinder of radius r the *divergenceless* perturbed field consistent with torque balance (9) and Ampére's law can be expressed as an expansion of the type

$$\mathbf{b} = \sum_{m,n} b_{//}^{m,n} e^{i(m\theta - nz/R + \varphi_{m,n})}\mathbf{e}_{m,n} + \sum_{m,n} C_{m,n}\nabla\psi^{m,n} e^{i(m\theta - nz/R + \varphi_{m,n})} \wedge \mathbf{e}_{m,n} \tag{10}$$

where the Fourier coefficients are expressed in terms of a scalar flux function

$$\psi = \sum_{m,n} \psi^{m,n} e^{i(m\theta - nz/R + \varphi_{m,n})} \tag{11}$$

where $y^{m,n}$ is a real amplitude and $j^{m,n}$ its phase. Moreover $\psi^{-m,-n} = \psi^{m,n}$ and $\varphi^{-m,-n} = -\varphi^{m,n} + \pi$ ensure that $\mathbf{b}$ is real.

The metric coefficients $C_{m,n}(r) = \left(m^2 + n^2\varepsilon^2\right)^{-1/2}$ and the "parallel" amplitude $b_{//}^{m,n} = C_{m,n}\sigma\psi^{m,n}$ are determined by the condition $\nabla \cdot \mathbf{b} = 0$

Consequently the explicit perturbed field components for m,n≠0 are to all orders in ε

$$b_r^{m,n} = \mathbf{b}^{m,n} \cdot \mathbf{e}_r = \frac{i}{r}\psi^{m,n} \tag{12}$$

$$b_\theta^{m,n} = \frac{1}{m^2 + n^2\varepsilon^2}\left[-m\frac{d\psi^{m,n}}{dr} + n\varepsilon\sigma\psi^{m,n} + n\varepsilon g\frac{G^{m,n}}{F^{m,n}}\psi^{m,n}\right] \tag{13}$$

$$b_\varphi^{m,n} = \frac{1}{m^2 + n^2\varepsilon^2}\left[n\varepsilon\frac{d\psi^{m,n}}{dr} + m\sigma\psi^{m,n} + mg\frac{G^{m,n}}{F^{m,n}}\psi^{m,n}\right] \tag{14}$$

Here $F^{m,n} = mB_{0\theta} - n\varepsilon B_{0\phi}$ and $G^{m,n} = mB_{0\phi} + n\varepsilon B_{0\theta}$. Note that m, n are integers.

For the present purposes we specialize the above expressions to the tokamak ordering in $\varepsilon_0 = a/R$ m,n = O(1), $\frac{B_{0\theta}}{B_{0\phi}} = O(\varepsilon_0)$, $\sigma = O(\varepsilon_0)$ and may neglect the finite pressure gradient term $g \approx \beta/a = O(\varepsilon_0^2)$. However contributions for which |m |<<|ne| must be considered with care

For |m |>|ne| we have:

$$G^{m,n} \approx mB_{0\phi} : \quad F^{m,n} = mB_{0\theta} - n\varepsilon B_{0\phi} \approx o(\varepsilon_0) \tag{15}$$

$$b_\theta^{m,n} \cong -\frac{1}{m}\frac{d\psi^{m,n}}{dr} \tag{16}$$

$$b_\varphi^{m,n} = \frac{1}{m^2}\left[n\varepsilon\frac{d\psi^{m,n}}{dr} + m\sigma\psi^{m,n} + mg\frac{G^{m,n}}{F^{m,n}}\psi^{m,n}\right] \approx o(\varepsilon_0)b_\theta^{m,n} \tag{17}$$

But for m=0 a strong scaling of the field perturbation with ε^{-1} appears

$$F^{0,n} = -n\varepsilon B_{0\phi} : \quad G^{0,n} = n\varepsilon B_{0\theta} \approx o(\varepsilon_0^2) \tag{18}$$

$$b_\theta^{0,n} = \frac{1}{n\varepsilon}\left[\sigma\psi^{0,n} + g\frac{G^{0,n}}{F^{0,n}}\psi^{0,n}\right] \cong \frac{\sigma}{n\varepsilon}\psi^{0,n} \tag{19}$$

$$b_\varphi^{0,n} = \frac{1}{n\varepsilon}\frac{d\psi^{0,n}}{dr} \tag{20}$$

The **b** field is a real quantity, so we can write

$$b_r(\mathbf{r},t) = -\sum_{m,n\neq 0} \frac{\psi^{m,n}(r)}{r}\sin\left(m\theta - n\phi + \varphi^{m,n}\right) \tag{21}$$

$$b_\theta(\mathbf{r},t) = \sum_{m,n\neq 0} b_\theta^{m,n}\cos\left(m\theta - n\phi + \varphi^{m,n}\right) \tag{22}$$

$$b_\phi(\mathbf{r},t) = \sum_{m,n\neq 0} b_\phi^{m,n}\cos\left(m\theta - n\phi + \varphi^{m,n}\right) \tag{23}$$

It is easy to show that in the formula (6)

$$B_0 = \sqrt{B_{0\phi}^2 + B_{0\theta}^2} \tag{24}$$

and

$$\left\langle e_\phi \cdot \nabla \cdot \Pi \right\rangle = \frac{\pi^{1/2} p_i}{R_0 v_{Ti}} V_\phi \sum_{m,n\neq 0} \frac{\left(B_{0\theta} b_\theta^{m,n} + B_{0\phi} b_\phi^{m,n}\right)^2}{B_0^4} \cdot \frac{n^2 q}{|m - nq|} \tag{25}$$

Therefore the general expression for toroidal viscous force arising from helical perturbations is

$$b^{m,n} = \left(\frac{B_{0\theta}}{B_0^2} b_\theta^{m,n} + \frac{B_{0\phi}}{B_0^2} b_\phi^{m,n}\right)\cos\left(m\theta - n\phi + \varphi^{m,n}\right) \tag{26}$$

Considering now the tokamak ordering with $m, n = O(1)$ we have for $m\pi 0$ the following contribution to the toroidal viscous force is

$$\left\langle e_\phi \cdot \nabla \cdot \Pi \right\rangle_{m\neq 0} \cong \frac{\pi^{1/2} p_i}{R_0 v_{Ti}} V_\phi \sum_{m\neq 0, n\neq 0} \varepsilon^2 \left(\frac{\psi^{m,n}}{r B_\phi}\right)^2 \cdot \left[\frac{\sigma r}{m\varepsilon} + \frac{gr}{\varepsilon^2}\frac{q}{m - nq} - \frac{m - nq}{m^2 q}\frac{r}{\psi^{m,n}}\frac{d\psi^{m,n}}{dr}\right]^2 \cdot \frac{n^2 q}{|m - nq|} \tag{27}$$

Note that the quantity in the squared bracket is O (1). In the vicinity of the rational surfaces there are helical current sheets related to the jump in $d\psi^{m,n}/dr$ and the radial current perturbation is negligible; in this limiting case Ampere's law gives $b_\varphi^{m,n} \approx -(n\varepsilon/m) b_\theta^{m,n}$ (see also Ref. 12) that in Eq. (26) cancels the $b_\theta^{m,n}$ contribution. The residual term $\propto g$ presents an apparent singularity; however in the non-linear stage with a magnetic island, due to the pressure profile flattening (p'=p"=0) across the island width it is expected that $g \approx (m - nq)^2$. Then to this order the viscous force *in the island region* would vanish, but non resonant components (m<0, n>0, and m>0, n<0) in the summation would still give a contribution.

For m=2,n=1 the contribution to this viscous force due to the $b_\theta^{m,n} \cong -\frac{1}{m}\frac{d\psi^{m,n}}{dr}$

term influences a region of plasma substantially wider [8] that the island formed at reconnection at the rational surface as can be seen qualitatively from Figs. (16) and (17) contributing to damping of rotation over a wide radial interval.

A more significant effect is due to the m=0 perturbations for which we have obtained different expressions. In this case (19) and (20) give for the m=0 contribution to the toroidal viscous force the expression

$$\left\langle e_\phi \cdot \nabla \cdot \Pi \right\rangle_{m=0} = \frac{\pi^{1/2} p_i}{R_0 v_{Ti}} V_\phi \sum_{n\neq 0} \frac{1}{|n|\varepsilon^2} \left(\frac{d\psi^{0,n}/dr}{B_\phi} \right)^2 \equiv K \cdot V_\phi \tag{28}$$

If we assume constant kinetic terms, also the quantity K is constant across the minor radius. In fact for m=0 the marginal stability mode condition (9) reduces to

$$\frac{d}{dr}\left(\frac{1}{r} \frac{d\psi^{0,n}}{dr} \right) = 0 \quad \rightarrow \quad \psi^{0,n} = A^{0,n} + B^{0,n} r^2 \tag{29}$$

$A^{0,n}$=0 in order to avoid a singularity of the radial field at r=0 (see definition (12)). Therefore we have:

$$K = \frac{4\pi^{1/2} p_i}{R_0 v_{Ti}} \sum_{n\neq 0} \frac{1}{|n|\varepsilon_0^2} \left(\frac{\psi^{0,n}(a)}{a B_\phi} \right)^2 \tag{30}$$

with $\varepsilon_0 = a/R$. The neoclassical viscous force is associated to the damping time scale $\left\langle e_\phi \cdot \nabla \cdot \Pi \right\rangle / \rho V_\phi$. A comparison between Eqn. (27) and (30) shows that the m=0 contribution to the neoclassical viscous force is a factor $O(1/e^4)$ greater than the mπ0 term. Asssuming typical JET values e=0.37, T_i=3KeV and a normalized perturbation $\psi / aB_\phi = 10^{-3}$, which is actually the maximum reasonable value,for the mode resonant at the q=2 surface (therefore adding both the harmonics m=2, n=1 and m=-2, n=-1) the damping time scale is of several second, which is too long. While the same calculation for the m=0, n=1 and m=0, n=-1 modes brings the time scale to~ 50 ms.

Moreover the m=0 term produces a uniform influence across the minor radius, which virtually explains the global braking of the plasma velocity, while the mπ0 term varies substantially with r. As shown in Fig.2 the mode spectrum produced by the saddle coils contains m=0 harmonics with non negligible amplitudes. Therefore the neoclassical viscous force associated to the m=0 modes is a good candidate to explain the experimental braking data. The flux-surface averaged equation of motion along the toroidal direction is then written as

$$r\rho \frac{\partial \omega_\phi}{\partial t} - \frac{\partial}{\partial r}\left[\mu_\perp r \frac{\partial \omega_\phi}{\partial r} \right] + rK\omega_\phi = rS_\phi / R_0^2 + \frac{T_\phi}{4\pi^2 {R_0}^3} \tag{31}$$

where $\omega_f = V_f/R_0$ is the toroidal angular velocity, T_f the flux-surface integrated electromagnetic torque and S_f a momentum source, which provides the equilibrium velocity profile ω_0:

$$\frac{\partial}{\partial r}\left[\mu_{\perp} r \frac{\partial \omega_0}{\partial r}\right] + r S_{\phi} / R_0^2 = 0 \tag{32}$$

Assuming $\rho, \mu_{\perp}$ constant and considering that the electrodynamic torque is rensonantly peaked on the the q=2 rational surface then for the bulk of the plasma outside $T_{\varphi} \cong 0$. The experimental data during the braking phase suggest a separable solution of equation (31):

$$\omega_{\phi}(r,t) \cong \omega_0(r) \cdot y(t) \; ; \;\; y(0) = 1 \tag{33}$$

Thus

$$\frac{dy}{dt} + \frac{K}{\rho} y + (y-1) \frac{S_{\phi}}{R_0^2 \rho \omega_0} = 0 \tag{34}$$

Note that the m=0 modes gives just a K constant with r. Defining $S_{\phi} / R_0^2 = \alpha \mu_{\perp} \omega_0$, from (32) one gets $\alpha = \left(j_{0,1} / a\right)^2$, $j_{0,1}$ being the first positive zero of the Bessel function J_0. So we can write (34) in the form

$$\frac{dy}{dt} + \frac{y}{\tau_D} + \frac{y-1}{\tau_{\mu}} = 0 \tag{35}$$

where $\tau_D = \rho / K$, and $\tau_{\mu} = \dfrac{\rho a^2}{\mu j_{0,1}^2}$. The consistency of this equations implies that the coefficients are independent of r. Note that the m=0 modes gives just a K constant with r and we have assumed also K independent of time. The solution of (35) is

$$y(t) = \frac{\tau_{\mu}}{\tau_{\mu} + \tau_D} e^{-t\left(\frac{1}{\tau_{\mu}} + \frac{1}{\tau_D}\right)} + \frac{\tau_D}{\tau_{\mu} + \tau_D} \tag{36}$$

A necessary condition for substantial slowing down of the plasma is

$$\tau_D \le \tau_{\mu} \tag{37}$$

In this case the time asymptotic value of Eq.(36) is $y_{brak} \le 1/2$ and the exponential braking time is

$$\tau_{brak} = \left(\frac{1}{\tau_{\mu}} + \frac{1}{\tau_D}\right)^{-1} \le \tau_{\mu} / 2 \tag{38}$$

which are both consistent with the experimental observations. shown in Figs.(8) and (9). As can be seen from (30) the dominant contributions to K comes from the n=1 and n=-1 harmonics. Adding these two terms the criterion (37) becomes

$$\frac{\psi^{0,1}(a)}{a B_{\phi}} \ge \frac{\varepsilon}{2\pi^{1/4}} \sqrt{\frac{R}{v_{Ti} \tau_{\mu}}} \tag{39}$$

An estimate with the values e=0.37, T_i=3KeV, t_m=0.5s, brings $\psi^{0,1}/\left(aB_\phi\right) \geq 3.8\cdot 10^{-4}$, which is indeed in qualitative agreement with experiment. Moreover the inclusion of higher toroidal harmonics in K increases the braking effect and lowers this threshold. An apparently similar slowing down of plasma rotation associated with a Transit Time Magnetic Pumping (TTMP) effect of non resonant helical field has been reported in the DIII-D tokamak [3,21].

IV. MODE UNLOCKING AND SPIN-UP

In about 50% of cases, after the external field is turned off, removing the electromagnetic braking torque, the locked mode is observed (on Mirnov coils signals) to spin up in the e- or i- drift direction by viscous restitution of momentum by the rest of the plasma. Simultaneously the island decays away on a resistive time scale since it is no longer driven by the external field and it is damped by the effect of the eddy currents generated in the vessel wall. A simple interpretation is given in terms of the standard Rutherford model [14] for the evolution of magnetic islands of width $W_{m,n} \propto \sqrt{rb_r^{m,n}}$, that after switch off of external fields is governed by the equation:

$$0.822\tau_R \frac{d\left(W_{m,n}/r_s\right)}{dt} = \left[\Delta_0' r_s - 2m\left(\frac{r_s}{d}\right)^{2m} \frac{(\omega\tau_w)^2}{1+(\omega\tau_w)^2}\right] \qquad (40)$$

Here island rotation effects and resistive wall boundary conditions [2] are included. In the customary notation m, n are the mode numbers, Δ'_{0m} and ω the tearing mode instability index and island rotation frequency, r_s and d the rational surface and vessel minor radii and τ_R, τ_w the plasma and vessel wall resistive time constants. The last term on the r.h.s represents the wall eddy current effect on the mode amplitude.

Before the application of the external field , for $0 < t < t_{on}$, the plasma can be assumed to be (marginally) stable, with for all W .

With the external field ramp forced reconnection eventually occurs at a critical value of the external current I_E and mode grows to a forced saturation amplitude W_{s1} where

After turn off of external field ramp the locked mode with amplitude W_{s1} finds itself again with and decreases as it spins, due to the wall eddy currents term . The decay of the velocity shift profile during spin-up can then be explained in elementary terms considering the solution of equation (34) when the external torques due to the external field are off:

$$\frac{d(y-1)}{dt} + (y-1)\frac{1}{\tau_\mu} = 0 \qquad \text{for} \quad t \geq t_{off} \qquad (41)$$

that gives explicitely

$$\omega_{Mirnov} \approx \omega_{t_{off}} + \omega_0 \frac{\left(t - t_{off}\right)}{\tau_\mu} \qquad (42)$$

If there is a mode in the laboratory frame its observed magnetic Mirnov signal frequency is ω_{Mirnov} and if the plasma is rotating toroidally with frequency ω then $\omega_{Mirnov} = \omega$

From Fig.3 it appears that at $t = t_0$, before mode onset, $\omega_{Mirnov_0} = 0$ but $\omega = \omega_0 = V_{\varphi 0}/R$, while at the end of the braking ramp, $t = t_{off}$ the plasma rotation plasma rotation is $\omega_{t_{off}} << V_{\varphi 0}/R$ (but not completely vanishing, in general) .

Then from the equation (42), in the laboratory frame we get , shortly after $t > t_{off}$:

$$\omega_{Mirnov} \approx \omega_{t_{off}} + \omega_0 \frac{(t - t_{off})}{\tau_\mu} \tag{43}$$

Therefore the spin-up difference from the initial frequency can be positive (e-drift) or negative (i-drift) according with the sign difference between $\omega_{t_{off}}$ and ω_0.

In the frame of reference of vanishing electric drift, defined by

$$\omega_E = \frac{E_r}{B_\theta R} = \frac{V_\varphi}{R} - V_\theta \frac{B_\phi}{RB_\theta} + \frac{1}{en_i RB_\theta}\frac{\partial p_i}{\partial r}$$

the mode frequency is $\omega' = \omega_{Mirnov} - \omega_E$ and from eq. 43) one has

$$\omega' \approx -\omega_E + \omega_{t_{off}} + \omega_0 \frac{(t - t_{off})}{\tau_\mu}$$

Therefore in this frame the sign of the mode frequency may depend on the amount of pressure and temperature flattening in the island region at $t \geq t_{off}$.

The partition of e- and i- drift cases according to magnetic field illustrated in Fig. 18 does not appear to have a causal relation with the threshold for reconnection.

CONCLUSION

A series of systematic experiments with external “error field” in JET has led to the reassessment and understanding of the empirical scaling laws governing the onset of “error field” locked modes and has shed light on the important physics of plasma rotation braking associated with a toroidal viscous drag originating from broken axisymmetry. In particular a very satisfactory match of basic theoretical concepts with data has been achieved, namely concerning the non-linear mode amplification occurring after slowing down to half the original frequency, and a direct test of a new theory of global plasma braking associated with helical modes has been provided. For ITER-like devices operating at a high fraction of the Greenwald density limit $n_G \propto I_p/\pi a^2 \propto B_\varphi/qR$ the empirical scaling obtained takes the form $b_{pen}/B \propto B^{-0.69}\omega_0^{0.5}$ that shows a mild, favorable effect of driven plasma rotation in raising the threshold for locked mode onset. On the other hand the potential danger of the anomalous braking discussed above and of its consequences can be enhanced by the natural occurrence of (0,n) perturbed components of the magnetic field due to strong elongation and shaping of the plasma cross section [6].

This work was performed under the European Fusion Development Agreement and was partly funded by Euratom , the UK Department of Trade and Industry and the Italian Consiglio Nazionale delle Ricerche .

REFERENCES

[1]. R. Fitzpatrick, T. Hender Phys. of Fluids B **31,** 1003 (1991)

[2]. T.C. Hender, R. Fitzpatrick a.W. Morris P.G.Carolan, R. D. Durst T. Edlington, J. Ferreira, S.J. Fielding, P.S. Haynes, J. Hugill, I.J. Jenkins, R.J. La Haye, B.J. Parham, D.C. Robinson, T.N. Todd, M. Valovic, G. Vayakis, Nucl. Fus. **32** ,2091 (1992); P. Leahy , P.G. Carolan, R.J. Buttery, K.D. Lawson ," The role of plasma rotation in error field scalings" *in Proceed. of the 26th EPS Conf. on Contr. Fusion and Plasma Physics, Maastricht, 14 - 18 June 1999 ECA Vol.23J (1999) 157 – 160*

[3]. R.J. La Haye, A.W. Hyatt, T.J. Scoville, Nucl. Fus . **32**(12), 2119 (1992)

[4]. R.J.Buttery, M.De Benedetti, T.C. Hender, B.J. Tubbing, Nucl.Fus. **40**(4), 807 (2000)

[5]. A.Gibson and the JET Team, Phys.of Plasmas **5**, 1839 (1998)

[6]. R. Aymar, V.A. Chuyanov, M. Huguet, Y. Shimomura, ITER Joint Central Team, ITER Home Teams, Nucl.Fus. **41**, 1301 (2001)

[7]. D.Stork et al in *Proceed. of the 14th EPS Conf. on Plasma Physics and Contr. Fus., Madrid, 1987,ECA Vol.I, (1987) 306-309*

[8]. A.I.Smolyakov, E.Lazzaro et al. Phys. Plasma, **2** (5), 1525 (1995)

[9]. A. Tanga, E. Lazzaro et al. Nucl. Fus. **17**,1877 (1987)

[10]. Wesson J.A.,Gill , M.Hugon , F.Sch¸ller , J.Snipes , D.Ward , D.Bartlett , D.Campbell, P.Duperrex , A.Edwards , R.Granetz ,N.Gottardi, T.Hender , E.Lazzaro,P.Lomas,N.Lopez-Cardozo,F.Mast,M.N.Nave,N.Salmon , P.Smeulders , P.Thomas , B.Tubbing , M.Turner, A.Weller, Nucl.Fus. **29**, 641 (1989)

[11]. A.Santagiustina,S.Ali Arshad,D.J.Campbell,G.D'Antona, M.Debenedetti, A.M. Edwards ,G. Fishpool, E. Lazzaro, R.J.la Haye, A.W.Morris ,R.Ostrom, L. Rossi,F. Sartori, P.Savrukhin, M.Tabellini ,A. Tanga , G.Zullo , "Studies of Tearing Mode Control in JET",in *Proceed.of the 22th EPS Conference on Controlled Fusion and Plasma Physics, Bournemouth, 26-30 July 1995 ECA Vol.18c IV(1995) 461-464*

[12]. R.Fitzpatrick Nucl. Fus. **33** (7) 1049 (1993)

[13]. E.Lazzaro et al Phys.of Plasmas **4,** 4017 (1997)

[14]. P.H. Rutherford , Phys.Fluids **16**, 1903 (1973)

[15]. H.R. Hicks et al. Journ. of Comput. Phys. **44** 46 (1981)

[16]. B.B. Kadomtsev in "The tokamak as a complex system ", Institute of Physics Publishing, Bristol 1987

[17]. K.C.Shaing e S.P. Hirshman, J.D.Callen, Phys.of Fluids **29,** 521 (1986)

[18]. W.F. Hughes, F.J. Young: "Electromagnetodynamics of Fluids", John Wiley & Sons, Inc, New York, 1966

[19]. R. Fitzpatrick, Phys. Plasmas **6**, 1168 (1999)
[20] W.A. Newcomb , Ann.Phys. (N.Y.) **10**, 232 (1960)
[21] R.J. la Haye ," Control of Neoclassical Tearing modes in DIII-D", in *Bull. 43rd Am. Phys. Soc, Div. of Plasma Phys. Ann.Phys. Long Beach. Ca.,Oct.29-Nov.2, 2001*

Table I - *Relevant discharges numbers: values of toroidal field B in tesla , line averaged density $n_e(10^{19})$, external saddle coils current $I_E(A)$ at reconnection, initial toroidal angular frequency ω_0 (rad/s), spin-up toroidal angular frequency ω_{spin} (rad/s), plasma temperature $T_{e|q=2}$ (rad/s)at q=2 surface, neutral beam power (in MW)*

Pulse No:	B [T]	$n_e(10^{19})$	$I_E(A)$	ω_0 (rad/s)	ω_{spin} (rad/s)	$T_{e\|q=2}$ (eV)	P_{NBI} (MW)
52066	1	1.39	2200	2500	-8.29	348	0.9
52065	1.5	1.51	2275	2264	38	651	0.9
52068	2.0	1.93	2672	3092	-149	461	0.9
52069	2.0	1.89	2559	3028	167	476	0.9
53610	2.0	1.65		2242		862	0.9
52058	2.5	2.27	1744	3000	191	673	0.9
52059	2.5	1.99	1631		-825	795	0.9
52060	2.5	2.00	1735		-1071	705	0.9
52061	2.5	1.85	2243	3231	-990	910	0.9
52062	2.5	1.84	2844	4848	-1172	1082	1.8
52063	2.5	1 .86	2253	3199	-1426	637	0.9
52067	3.0	1.90	1849	2681	-1506	627	0.9

Table II - *Values of exponents of scaling law $b_{pen}/B \propto n^{a_n} B^{a_B} \omega_0^{\eta}$ for the normalized reconnection threshold and rotation frequency $\omega_0 \propto B^{\alpha} (P_{NBI}/n)^{\beta}$ in different experiments [3,4,13]. For JET–2000 the data of Fig. 7 are considered*

	a_n	a_B	α	β	η
COMPASS [2]	0.55	-2.2	n.a.	n.a.	1
JET-98 [4]	0.97	-1.2	n.a.	n.a.	0
JET-2000	0.58	-1.274	0.562	0.652	0.5
Theory Ideal-viscous regime [12]	2/3	-7/3			1/21
Visco-resistive regime [12]	7/12	-13/6			1

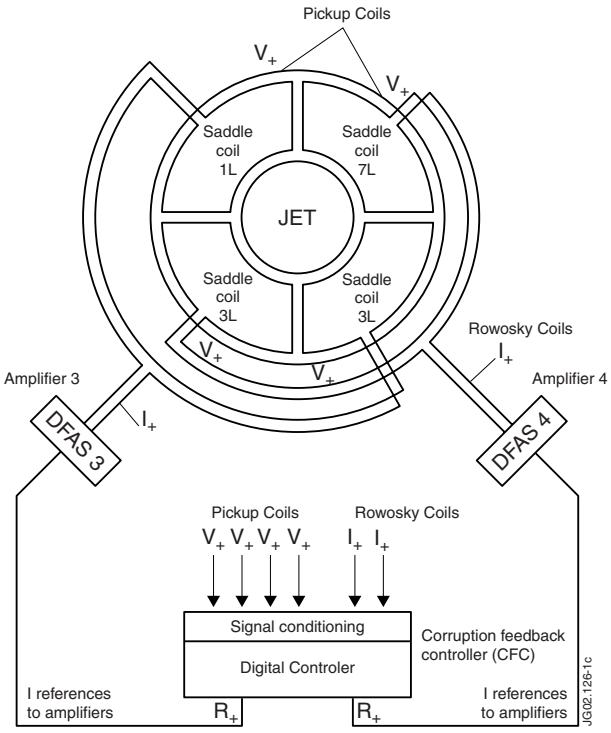

Figure 1: JET-Saddle coils system used in the experiments described. An external field with m.n helical components can be generated by suitable coil connections.

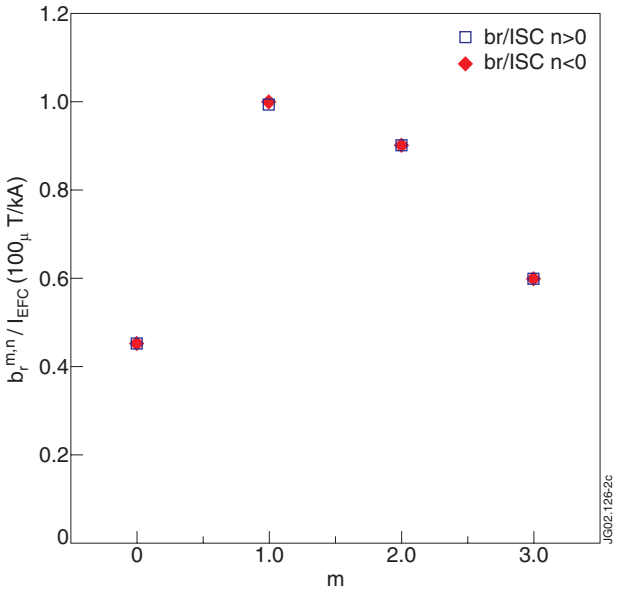

Figure 2: (m, n) external field component, normalized over saddle coils current vs. pitch numbers ratio m, n=1; open squares are for n>0, diamonds for n<0.

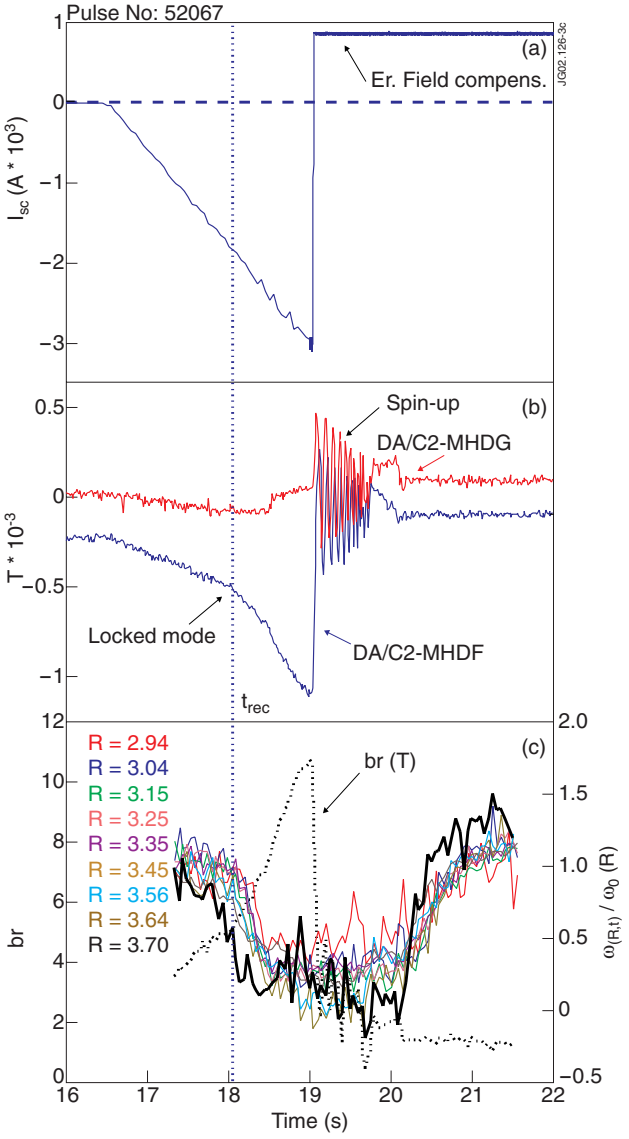

Figure 3: (a) Typical external magnetic field waveform; the coils current ramp here starts at t_0=16.4s after the discharge start time t=40.s; at end of ramp compensation of natural error field allows mode spin-up in e- or i-drift directions; (b) magnetic signals showing linear and non-linear response (t=18.04s); (c) charge exchange spectroscopy signals showing plasma rotation frequency at different radii normalised over frequency at the start time of the coils ramp. At field "penetration" sudden braking occurs

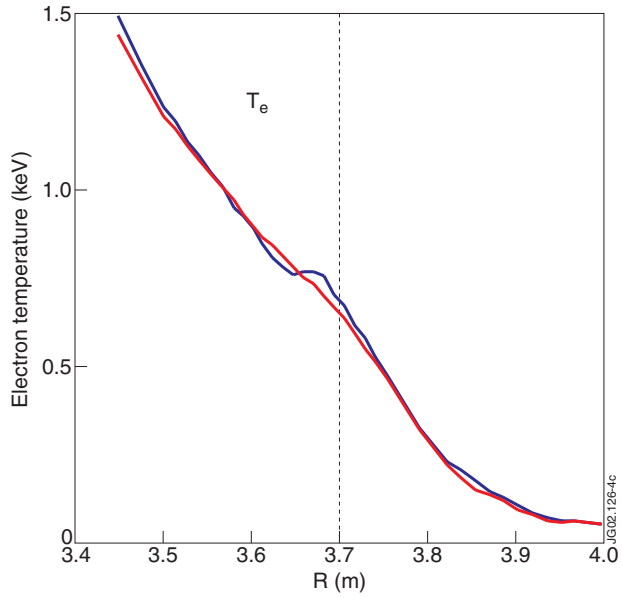

Figure 4: Temperature profile flattening in the region of the (2,1) island formed by driven reconnection (JET shot 52063)

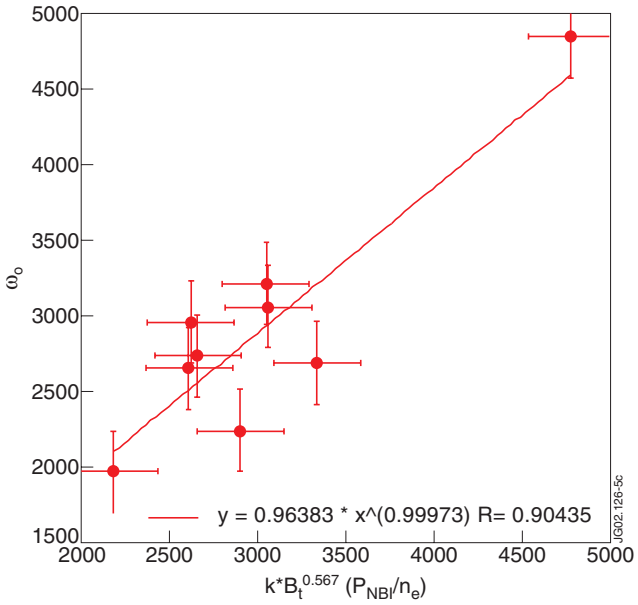

Figure 5: Power law scaling of the local angular rotation frequency $\omega_0 \equiv \omega(R = R_{q=2}, t_0)$ at the q=2 surface with n, B and P_{NBI}

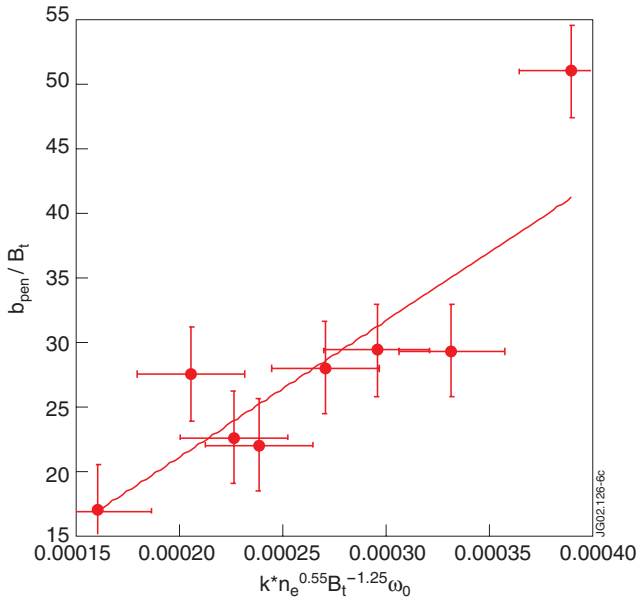

Figure 6: Scaling of the penetration threshold normalized over the toroidal field B vs power law $\sim n^{1/2}B^{-5/4}\omega_0$ where ω_0 is the local angular rotation frequency at the q=2 surface.

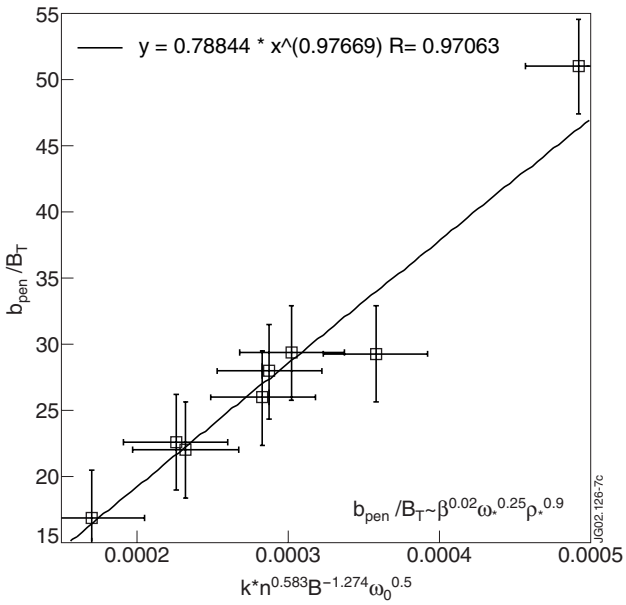

Figure 7: Scaling of the penetration threshold vs power law $\sim n^{0.58}B^{-1.274}\omega_0^{1/2}$ where ω_0 the local angular rotation frequency at the q=2 surface.

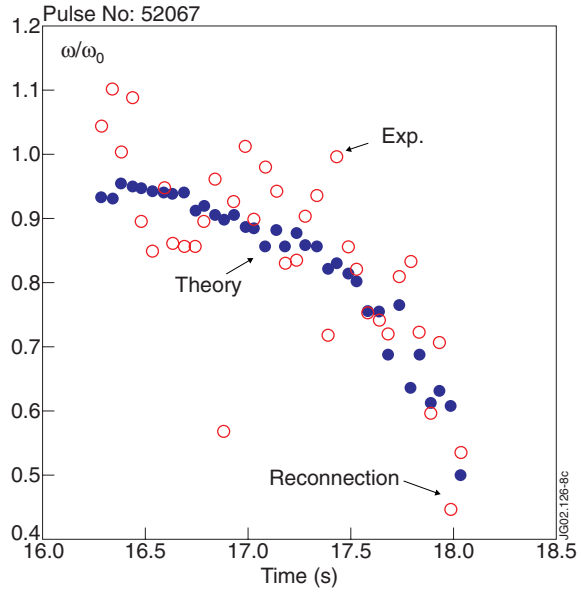

Figure 8: Braking of plasma toroidal rotation (charge exchange diagnostic) at the q=2 surface. Penetration occurs when the local angular rotation frequency at the q=2 surface is $\omega = \omega_0/2$. Full dots are the calculated values of theoretical formula (1); circles are the experimentally observed values of ω/ω_0. The coils current ramp starts at t_0=16.4s from the discharge start time t=40s.

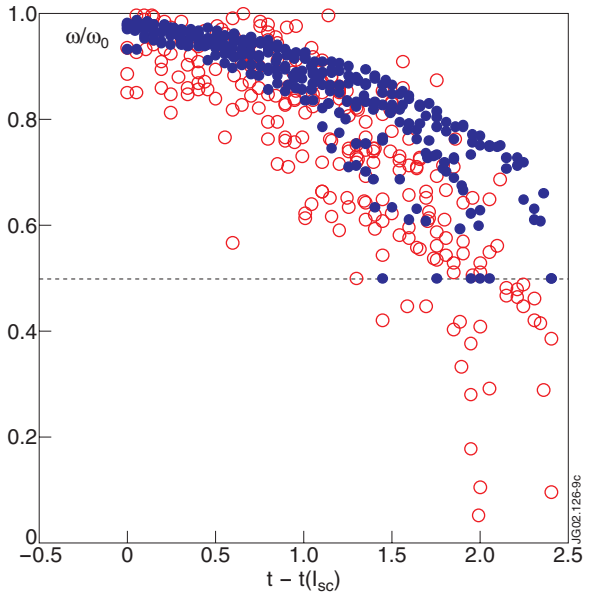

Figure 9: Occurrence of braking of plasma toroidal c) at the q=2 surface for all the discharges. Full dots are the calculated values of theoretical formula (1); circles are the experimentally observed values of ω/ω_0.

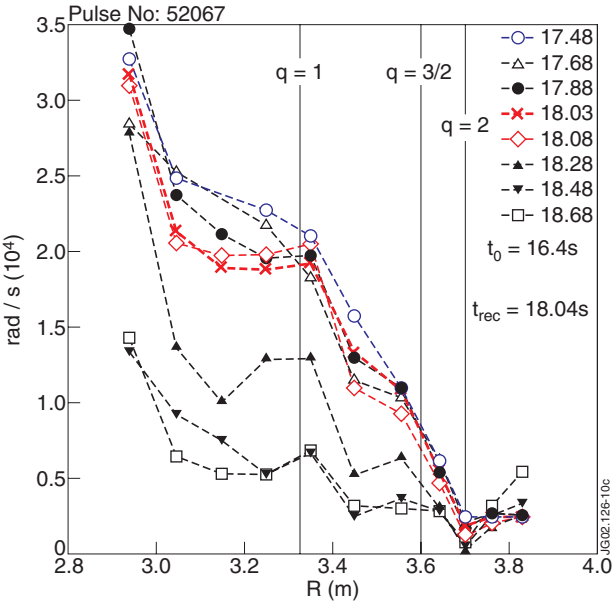

Figure 10: Experimental plasma toroidal angular velocity profile evolution. There is the clear evidence of the e.m. torque localization at q=2 surface and evidence of the global braking after island formation at t ~ 18.04s

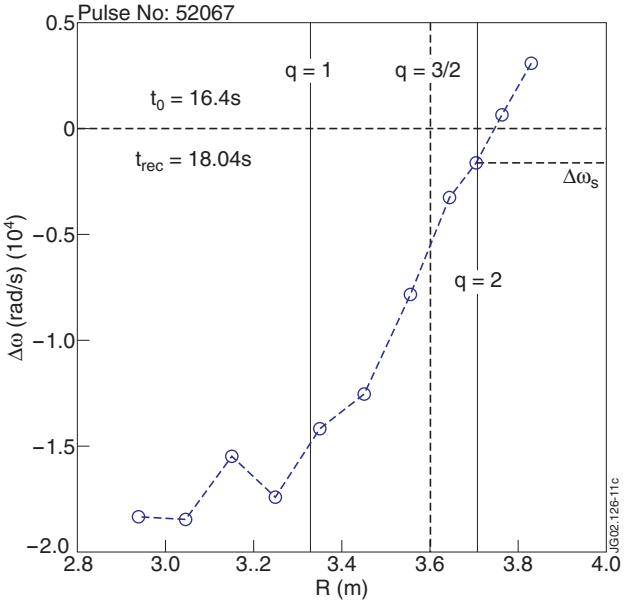

Figure 11: Profile of the toroidal angular velocity shift along the major radius R for Pulse No: 52067 at penetration time t~18.04 s. It is apparent that the no slip condition is violated. R=2.8 m is the machine axis.

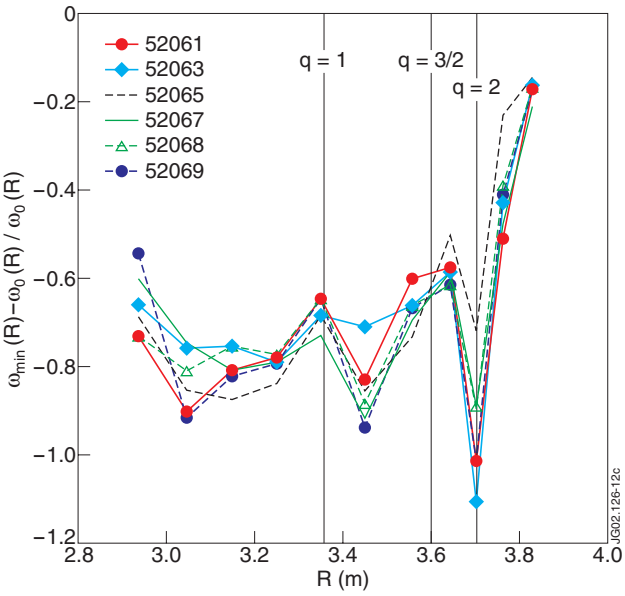

*Figure12: Profile of the **relative** toroidal angular velocity shift [ω_{min} (R) - ω_0 (R)]/ω_0 (R) (normalized over initial **profile**) for several discharges at time of island formation. R=2.8 m is the machine axis. It is apparent that the "no slip condition" is not met, as it would require constant toroidal angular velocity shift.*

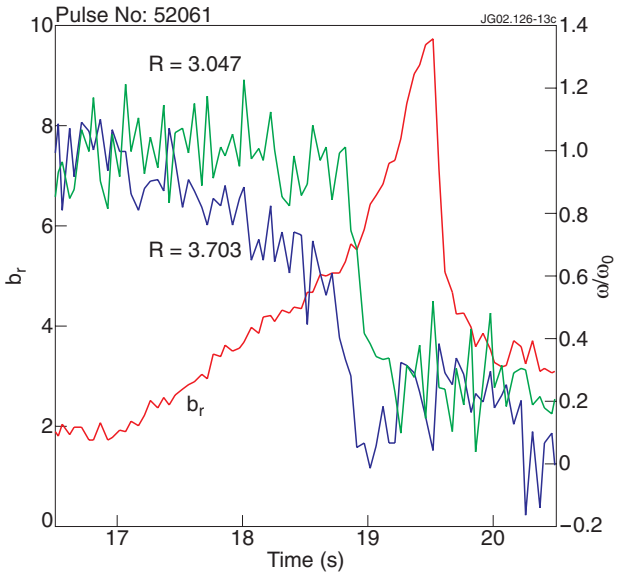

Figure13: Braking of rotation in JET Pulse No:0 52061

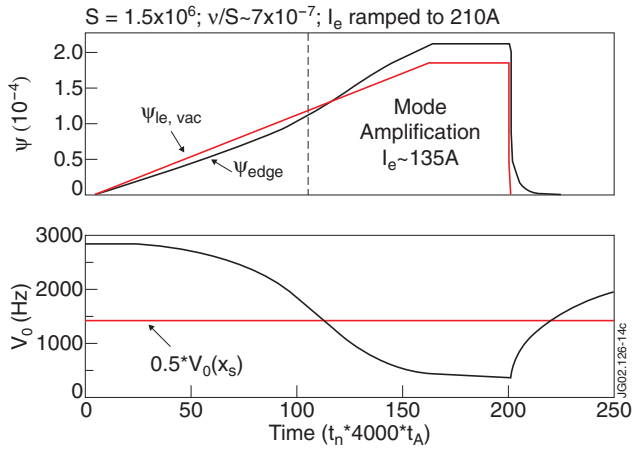

Figure 14: Theoretical RMHD model of driven reconnection of the helical flux ψ_s in presence of toroidal rotation. Non-linear mode amplification occurs when rotation velocity is halved. Here The velocity is indicated with in the units of the corresponding angular frequency and time is a multiple of Alfvén time.

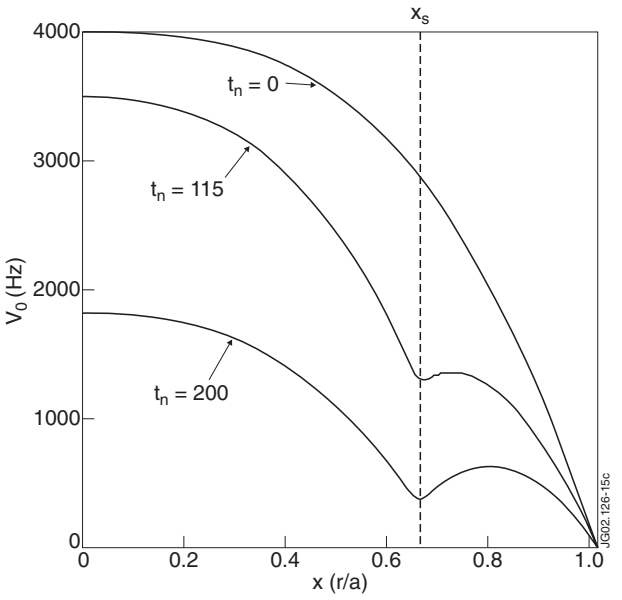

Figure 15:Theoretical model of evolution of the plasma toroidal rotation in presence of viscosity. The variation of the velocity profile is pretty much uniform, in contrast with the experimental data of Figs 10 and 11.

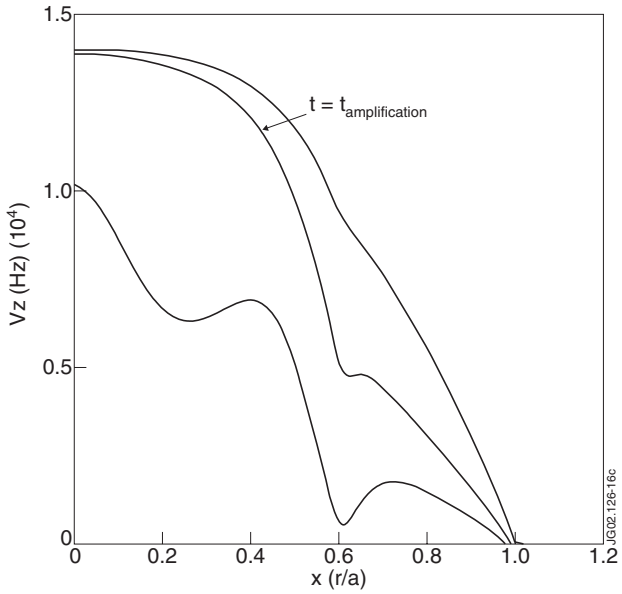

Figure 16: Theoretical model of evolution of the plasma toroidal rotation in presence of a braking effect $\propto|b_\theta|^2 V_\zeta$, in qualitative agreement with the typical experimental observations (e.g. Fig. 10)

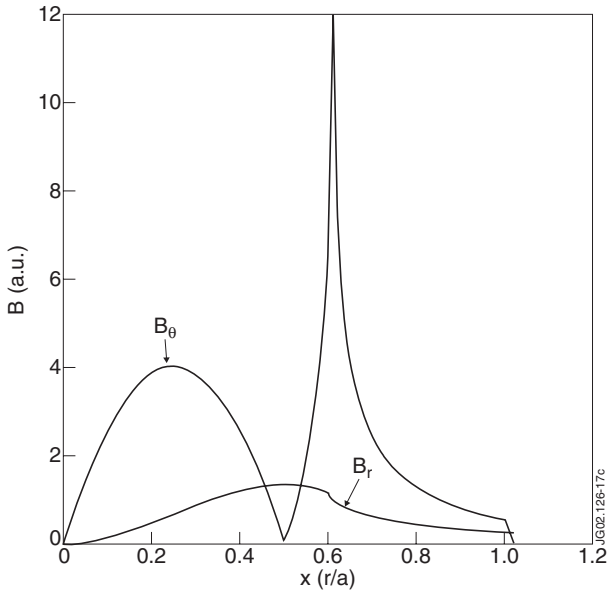

Figure 17: Radial extension of typical m=2, n=1 b_r and b_θ perturbations; the plasma toroidal rotation is affected by a a braking effect $\propto|b_\theta|^2 V_\zeta$, over a radial range wider than the island size (see Fig.15) .

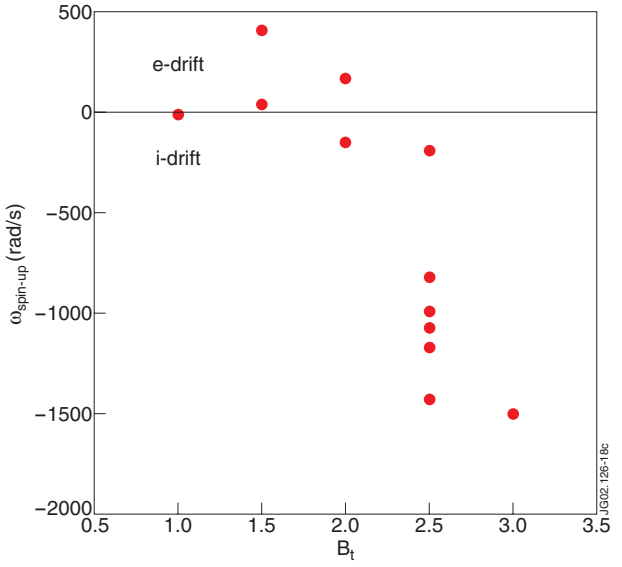

Figure 17: Partitioning of e-drift and i-drift modes according to B. The ordinates are the averaged mode spin-up angular frequencies of the Mirnov signals averaged and the abscissae are the values of toroidal field scanned in the experiment.